Natural hydroxy-isoflavone as potential modulator of Salmonella virulence, targeting the T3SS complex at host-pathogen interface

Varma Aryan, Tripathi Swati, Sahni Deepak, Bharati Akhilendra Pratap* and Sharma Chandresh*
School of Life Sciences and Biotechnology (SLSBT), Chhatrapati Shahu Ji Maharaj University, Kanpur, Uttar Pradesh, INDIA
*akhilendrapratap@csjmu.ac.in; chandreshsharma@csjmu.ac.in

Abstract

Salmonella are acquiring resistance to conventional antibiotics, comprising of fluoroquinolones providing limited treatment options to enteric fever. Similar to many Gram-negative bacteria, Salmonella pathogenicity island-1 (SPI-1) encodes Type Three Secretion System (T3SS), which forms invasosomes. T3SS needle complex at the host-pathogen interface allows Salmonella invasion proteins (Sips) to stimulate membrane ruffles and facilitate pathogen uptake through intimate attachment. Therefore, the present study intends to repurpose naturally derived small molecules against Sips, which may potentially block SPI-1-mediated virulence and inhibit Salmonella invasion. Invasosomes-associated target virulence factor (t2785) of S. typhi, was modelled through the SWISS-MODEL platform. A naturally derived compound library was used for screening based on their ligand binding affinity, adhering to designated grid coordinates. Data was analyzed and visualized post screening. Modelling of Sip from S. typhi revealed a 3D structure homologous to S. typhimurium Sip (PDB: 2YM9).

Screening resulted 7 promising hydroxyisoflavones, interacting with the receptor pocket, made up of negatively charged amino acids (D147, S148, T219 etc.). Among the binder hydroxyisoflavones, four demonstrated a stronger affinity towards structural Sip(s) involved in rearrangement and formation of the T3SS-needle complex. Hence, repurposed naturally derived small molecules against Sips, may impede T3SS complex at host-pathogen interface and potentially inhibit Salmonella invasion.

Keywords: *Salmonella*, Invavsomes, Hydroxisoflavones, Natural products, T3SS, SIP.

Introduction

Enteric fever, a systemic illness caused by the bacterium *Salmonella* enterica, serovar Typhi (*S. typhi*) and serovar, Paratyphi A (*S. paratyphi A*), poses a significant global health burden. This disease is strictly human-specific and is predominantly prevalent in regions characterized by overcrowding, inadequate sanitation and limited access to clean water, underscoring the urgent need for targeted eradication efforts[27,32]. It is estimated that *S. typhi* is responsible for approximately 25 million infections and 222,000 deaths annually worldwide[33]. Historically, antibiotics such as fluoroquinolones, ampicillin, co-trimoxazole, chloramphenicol and third-generation cephalosporins have been employed as first-line therapies for enteric fever[4,21].

However, Salmonella species have increasingly acquired resistance to these conventional antibiotics, particularly in developing nations, due to plasmid-mediated and chromosomal mechanisms[5,8]. Plasmid-mediated resistance to ampicillin, chloramphenicol and co-trimoxazole, combined with chromosomal mutations conferring resistance to fluoroquinolones, has severely limited the efficacy of these otherwise effective antibiotics[20]. The Type III Secretion System (T3SS) is a crucial virulence apparatus utilized by *Salmonella* to deliver effector proteins into host cells. Encoded by *Salmonella* Pathogenicity Island 1 (SPI-1), the T3SS machinery is indispensable for bacterial invasion[12]. Structurally, the T3SS is an intricate, needle-like apparatus that spans the inner and outer membranes of Gram-negative bacteria, providing a direct conduit for protein translocation from the bacterial cytoplasm into the host cytosol[36].

The external portion of the T3SS consists of a polymerized needle structure formed by 120 copies of the PrgI protein[26]. At the tip of the needle resides, the tip complex, is partially composed of the SipD protein. The SipD protein, comprising of 343 amino acid residues, features a prominent long central coiled-coil motif that gives it an oblong shape[9,17]. This coiled-coil structure is crucial for the assembly and stabilization of the T3SS apparatus, which is vital for bacterial virulence[10]. One key virulence mechanism is the ability to invade non-phagocytic intestinal epithelial cells. This invasion is mediated by a complex cluster of effector proteins including Sip proteins which facilitate the reorganization of the host cell actin cytoskeleton. This reorganization induces membrane ruffling, enabling bacterial internalization[19,23,24].

Given its essential role in Salmonella pathogenesis and its conserved structural features, the T3SS represents a promising target for therapeutic intervention. Through this study, an attempt has been made to target the Sip protein and its interactions within the needle apparatus, which may possibly disrupt the assembly and function of the T3SS, thereby attenuating Salmonella virulence and providing a novel strategy for combating antimicrobial resistance.

Material and Methods

***In silico* Sequence Analysis:** Invasosome-associated *S. typhi* Sip protein; the target virulence factor t2785 (Gene Accession ID AL513382.1) was identified and its amino acid sequence was obtained from the web-based protein database Uniprot (http://www.uniprot.org) (Q56136)[2]. Once the amino acid sequence [ML$(X)_{336}$QG] was retrieved and searched for the crystal data, subsequent step was to deduce or predict the three-dimensional (3D) structure of the Sip protein.

Modelling and structure analysis of Sip protein (t2785): A 3D model for Sip protein was prepared by the Swiss Model (https://swissmodel.expasy.org/) using a fully automated protein structure homology-modelling via Expasy Web server[37]. Briefly, aligning the target sequence with known protein structures deposited in the Protein Data Bank (PDB), subsequent homology between the target protein and template protein was used to generate a reliable, full-length target Sip protein 3D representation. While preparing 3D structure to be used for molecular ligand docking simulations to target Sip protein, several preparatory steps were undertaken, ensuring that the docking procedure accurately reflects the chemical environment of the protein. The predicted structure containing water molecules was removed from the model as they can interfere with docking studies. Further, for proper electrostatic interaction, Kollman charges (partial charges) and hydrogen atoms were assigned to the atoms in the protein structure, essential in protein-ligand binding.

Ligand Library Preparation and Screening: A ligand library was curated from two major databases: PubChem Database (https://pubchem.ncbi.nlm.nih.gov/) and ZINC Database (https://zinc.docking.org/)[16,18]. The ligands from these databases were selected based on their chemical properties, size and relevance to the study using SwissADME (http://www.swissadme.ch)[7]. A docking grid was defined on the receptor Sip protein to identify the binding site or pocket for ligand docking. The GRID box was decided through appropriate centered and size dimensions with defined X, Y and Z coordinates. The other GRID parameters included maximum number of binding modes (num_modes = 10) and an energy range (≈4 kcal/mol) to capture multiple conformations of ligands within the active site. Once selected, the ligand structures were converted into the PDBQT format using the Open Babel tool (https://openbabel.org/).

Molecular Docking Tools: The PDBQT format, essential for molecular docking calculations, which contained both atomic coordinates and charge information, was used to facilitate docking through the web-based tool AutoDock tools[1,5,7]. Docking simulations were conducted within predefined GRID box parameters. Docking scores were calculated, which represent the binding affinities of each ligand conformation in kcal/mol. In addition to the binding affinities, interaction metrics such as the root mean square deviation (RMSD) values were determined by comparing the experimental and predicted ligand structures, specifically focusing on the alignment of movable heavy atoms.

Additionally, lower bound (L.B.) and upper bound (U.B.) RMSD variants were computed to assess the accuracy of the docking predictions, which provide a range of acceptable deviations in atom placement during the distance calculations, reflecting different tolerances for structural matching. The most optimal binding conformations were selected based on the aforementioned parameters as indicators of prediction accuracy.

Visualization and Interaction Analysis: After completing the molecular docking simulations, the results were analyzed to identify key interactions between the ligands and the receptor Sip protein. The primary tool used for this analysis was Chimera (https://www.cgl.ucsf.edu/chimera/), Protein-Ligand Interaction Profiler and PyMol v3.1.3[1,29]. In particular, Chimera was used to identify hydrogen bond interactions as they play a critical role in ligand-receptor interactions. Moreover, 3D visualization of ligand-receptor interactions for identifying a docking pose, i.e. areas of the receptor crucial for binding, as well as ligand, might exhibit a strong binding affinity.

Ligand Binding Site Analysis: To further ensure that the ligands were binding in the correct region of receptor Sip protein, a web-based tool, ProteinPlus (Zentrum) (https://proteinplus.zentrum.ubc.ca/) was utilized for predicting the potential binding pocket and the key residues involved in ligand interactions on the target receptor Sip protein[11,34,35]. In addition to 3D visualization, Chimera and ProteinPlus were also used to generate 2D interaction diagrams for simplified representation of the binding interactions. These diagrams were particularly useful for visualizing hydrogen bonds, highlighting the donor and acceptor atoms involved in each interaction, hydrophobic and/or Van der Waals interactions and providing insights into the mechanisms that drive binding affinity.

Results

A predicted 3D Model for receptor Sip protein (t2785) generated: The amino acid (Uniprot ID Q56136) sequences of the *S. typhi* Sip protein were utilized to generate a predictive 3D structure (Figure 1). Swiss-Model, a fully automated protein structure homology-modelling tool on the Expasy Web server revealed a 3D structure of the *S. typhi* receptor Sip protein, which showed homology to *S. typhimurium* Sip8 (PDB: 2YM9), which is the closest serovar and infects humans (Figure 1).

The data for percentage homology (87.94%) and other parameters associated with the predictive 3D model of *S. Typhi* Sip protein have been represented in figure 1. The representation for predictive homology modelling by comparative 3D protein structure is shown in figure 1.

Ligand screening and docking revealing the significant interaction of hydroxyisoflavones with Sip protein: To discover significant binders among the sets of hit compounds, we curated a list of natural products harbouring 270 compounds with similar structures from two major databases, PubChem and ZINC and virtually screened them (Figure 2). A sequential docking pipeline involving different levels of exhaustiveness to screen a library of natural compounds resulted in the 7 best candidates for further detailed investigations through molecular docking simulations (Figure 2; Table 1).

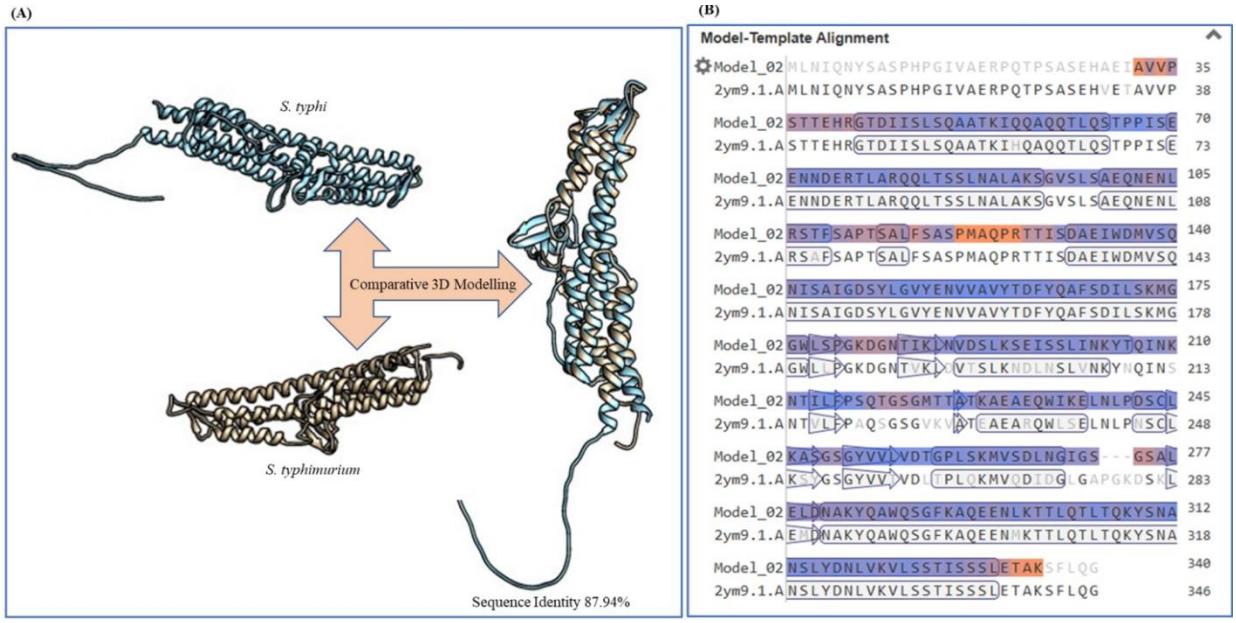

Figure 1: Homology Modelling of *S. Typhi* Sip protein (t2875): (A) Structural prediction of *S. typhi* based on its sequence alignment and homology with the known structure of *S. typhimurium*, depicting conserved regions and overall structural similarity. (B) Sequence comparison using Swiss-Model: Alignment of the *S. typhi* sequence with the *S. typhimurium* sequence showcasing similarity in Coiled-coil domain

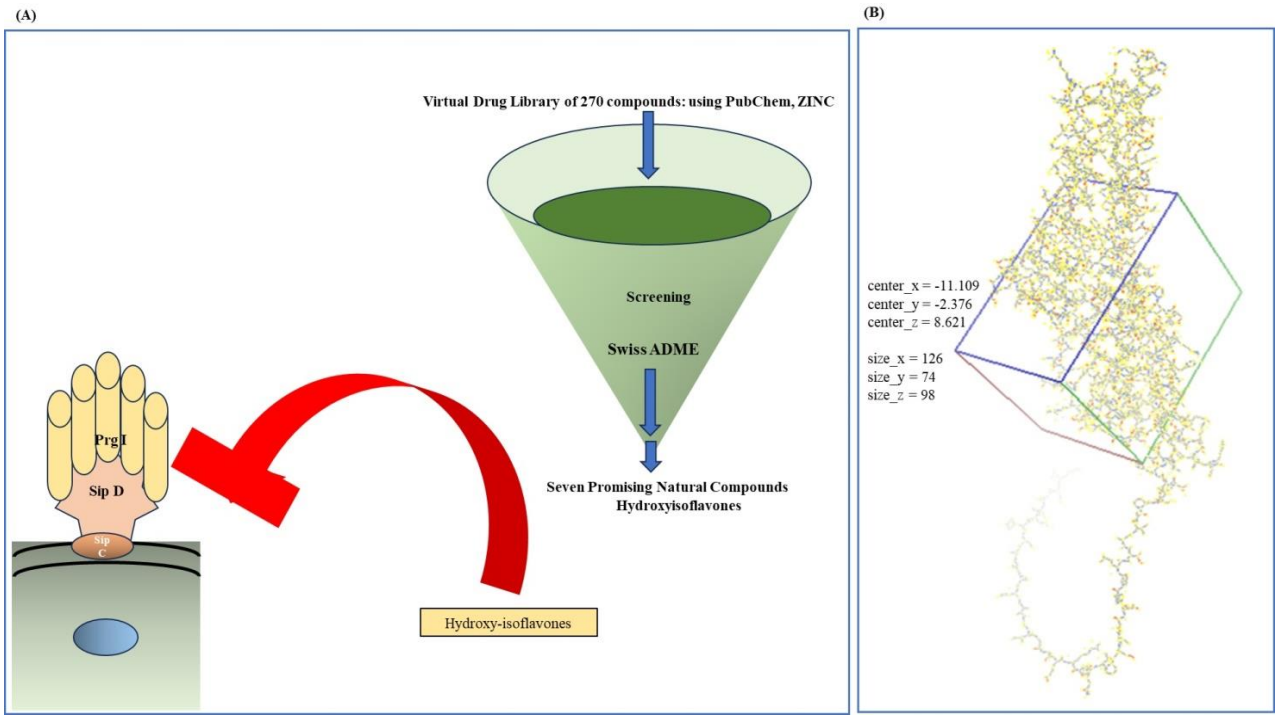

Figure 2: Overview of Library Construction and ligand Screening; (A) Assembly of virtual libray with 270 naturally derived compounds from PubChem and ZINC databases, followed by initial screening using the Swiss-ADME tool to evaluate drug-likeness and pharmacokinetic properties and its functionality (B) Visualization of the Sip target protein with the defined grid box created using AutoDock Vina, representing the docking space used for predicting ligand binding within the active site

Table 1
Interaction of screened ligand with receptor Sip proteins in different modes

S.N.	Compounds	Properties	Interaction modes									
			Mode 1	**Mode 2**	**Mode 3**	**Mode 4**	**Mode 5**	**Mode 6**	**Mode 7**	**Mode 8**	**Mode 9**	**Mode 10**
1	Biochanin A	Affinity (kcal/mol)	-8.5	-8.1	-8.1	-8.0	-8.0	-7.9	-7.4	-7.0	-6.9	-6.8
		RMSD (L.B.)	0	5.916	2.018	4.774	2.116	3.626	11.637	12.502	15.482	10.011
		RMSD (U.B.)	0	9.721	3.489	8.748	6.283	7.592	14.053	14.765	14.828	11.411
2	Formononetin	Affinity (kcal/mol)	-8.6	-8.0	-7.9	-7.5	-6.4	-6.4	-6.3	6.3	-6.3	-6.3
		RMSD (L.B.)	0	2.623	1.430	11.401	22.405	30.345	10.915	23.440	30.198	35.537
		RMSD (U.B.)	0	7.001	5.44	13.769	24.120	32.721	13.052	24.888	32.066	38.666
3	Luteolin	Affinity (kcal/mol)	-9.1	-8.9	-8.9	-8.8	-8.2	-7.9	-7.9	-7.6	-7.4	-7.2
		RMSD (L.B.)	0	1.535	1.534	1.044	10.843	10.674	2.154	15.104	13.793	7.362
		RMSD (U.B.)	0	2.238	2.800	1.978	13.072	12.718	4.068	16.592	14.793	15.452
4	Scopoletin	Affinity (kcal/mol)	-6.6	-5.8	-5.6	-5.5	-5.5	-5.4	-5.3	-5.3	-5.1	-5.0
		RMSD (L.B.)	0	15.941	12.852	14.711	29.018	22.152	28.470	34.219	34.007	17.702
		RMSD (U.B.)	0	16.981	14.261	16.058	30.242	22.858	29.792	34.897	36.251	19.290
	Ginistein	Affinity (kcal/mol)	-6.6	-5.8	-5.6	-5.5	-5.5	-5.4	-5.3	-5.3	-5.1	-5.0
5		RMSD (L.B.)	0	15.941	12.852	14.711	29.018	22.152	28.470	34.219	34.007	17.702
		RMSD (U.B.)	0	16.981	14.261	16.058	30.242	22.858	29.792	34.897	36.251	19.290
	Afrormosin	Affinity (kcal/mol)	-7.0	-7.0	-6.9	-6.6	-6.6	-6.5	-6.5	-6.5	-6.4	-6.4
6		RMSD (L.B.)	0	1.396	1.788	20.473	1.902	20.711	21.414	27.256	16.404	20.674
		RMSD (U.B.)	0	5.445	5.321	21.098	5.447	21.323	23.067	28.189	17.798	21.757
	Baptigenin	Affinity (kcal/mol)	-7.9	-7.5	-7.0	-6.7	-6.7	-6.7	-6.6	-6.6	-6.6	-6.5
7		RMSD (L.B.)	0	15.576	20.427	22.449	14.381	25.067	20.142	20.569	20.319	20.388
		RMSD (U.B.)	0	17.330	21.396	24.203	15.331	25.953	21.306	22.594	21.360	21.407

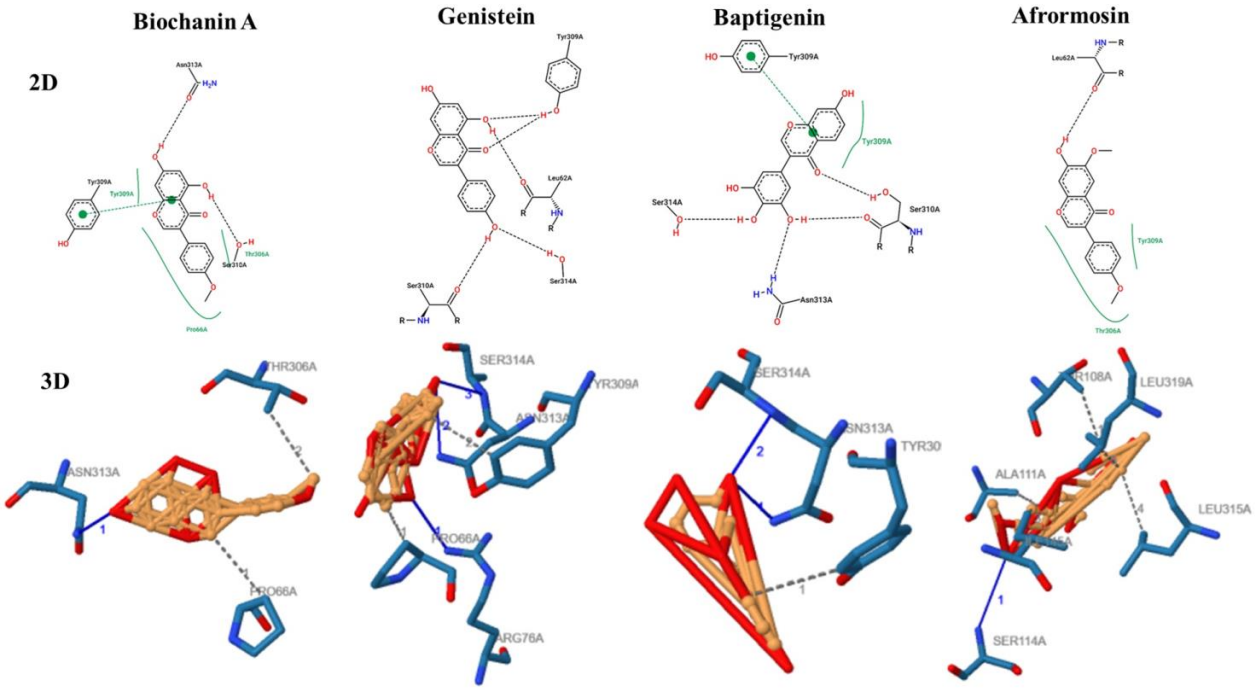

Figure 3: Summary of the interactions of four ligands—Biochanin, Genistein, Afrormosin and Baptigenin. Figure displays the 2D structure of with boundligand, along with the 3D interaction visualization, highlighting the amino acid interactions. Binding details include Biochanin interacting with T306, Genistein with T314, Afrormosin with T319 and Baptigenin also with T314. Binding affinities (in kcal/mol) indicate favourable hydrogen and hydrophobic bonding with distances (measured in Å) highlighting precise ligand-receptor engagement. These visualizations were generated using structural analysis tools ProteinPlus (Zntrum) for 2D interaction and 3D by Protein Ligand Interaction Profiler (PLIP), emphasizing critical binding interactions within the active site of the target protein.

Interacting ligands specifically bound to the Sip receptor protein, particularly targeting key amino acid residues in the binding pocket (critical for needle protein formation) (Figure 3 and 4; Table 2 and 3). Other non-specific interactions which contributed to overall binding stability (Figure 3 and 4; Table 2). Out of several binding conformations, Biochanin A exhibited strong hydrogen bonding with T306 of the Sip protein, with a bond distance of 3.72 Å with its 8th mode, suggesting stable binding (Figure 3; Table 3). Similarly, Genistine demonstrated binding at multiple positions with its seventh conformations showing hydrogen bonding with serine S314 of the Sip protein at distances of 3.34 Å respectively, indicating effective ligand-receptor interactions (Figure 3; Table 3).

Baptigenin, in its eighth conformation, interacted with serine S314 of the Sip protein at a distance of 3.01 Å, while Afrormosin bound to T319, of the Sip protein in eighth conformations, with bond distances of 3.53 Å (Figure 3; Table 3). Additionally, van der Waals interactions with specific residues like S148, Y149, E237, N239, T333 along with other stabilizing forces were observed within the receptor's binding pocket, further enhancing the stability of the ligand-receptor complexes mentioned in (Figure 3; Table 2 and 3).

Moreover, the results highlighted several ligands, particularly seven hydroxyisoflavones which displayed favourable binding affinities, zero RMSD values and consistent hydrogen bonding (Table 1 and 2). The first and most favourable conformations demonstrated strong interactions, including Luteolin (-9.1 kcal/mol, residues E70 and N73, Formononetin (-8.6 kcal/mol, residues E70 and N73), Biochanin A (-8.5 kcal/mol, residues S217) Genistein (-8.2 kcal/mol, residues E230), Baptigenin (-7.9 kcal/mol, residues D147), Afrormosin (-7.0 kcal/mol, residue S118, E230, F215, P216) and Scopoletin (-6.6 kcal/mol, residues N73,E70) (Table 1 and 2; Figure 4).

All ligands consistently bound within the same pocket across the 10 docking modes analyzed, further validating the reliability and functional importance of the identified binding pocket in ligand-receptor interactions. However, Luteolin, Formononetin and Scopoletin demonstrated binding at residues N73 and E70, exhibiting strong binding affinities. However, these residues are located in the N-terminal region of the protein and were therefore deemed insignificant for this analysis (Table 2; Figure 4). Furthermore, Scopoletin displayed binding at residue S148, but this interaction lacked corroboration from both 2D and 3D interaction visualization tools as detailed in table 2. As a result, these interactions were deemed unreliable and excluded from further evaluation as potential high-affinity binders. In a nut-shell among the binder hydroxyisoflavones, four, Biochanin A, Genistein, Baptigenin and Afrormosin, demonstrated a stronger affinity towards the structural Sip(s) involved in rearrangement, hence, depicting potential disruptor of the T3SS-needle complex.

Table 2
Comprehensive binding of hydroxyisoflavones to the different amino acid residues on the receptor Sip protein

S.N.	Compounds	Tools	Interaction modes									
			Mode 1	**Mode 2**	**Mode 3**	**Mode 4**	**Mode 5**	**Mode 6**	**Mode 7**	**Mode 8**	**Mode 9**	**Mode 10**
1	BIOCHANIN A	Protein Plus Zentrum (2D)	S217	D147, S217, P216	T108, I145, A111	D267, W287, A286, K283	Y309, T306	Q57	L116, S200	Y309, S310, N313, T306	K210, G220	S310, Y309, L62, N313, 66P
		PLIP (3D)	S217	216, S217	S114, L315, F117	D267, K283, A286	N313	L201, K204, I170		N313, T306, P66	K210, N209	S310, N313, T306, P66
		Chimera	E70	E70	T219,E70	-			S217, T224	Q63 , L62	T225, D147	G151, N155
2	FORMONONENTIN	Protein Plus Zentrum (2D)	E70, N73, N211	T77, N155	S148, E230, V152	A111, I145, T108, F117	A123, R126, E133	E230, P216			D267, K283, A286, W287	D147, S217, T219
		PLIP (3D)	N73, T77,	N73, T77	E230, S217	A111, S114	R126,T127	P216, T224	P260	R106,S110	D267,K283	D147, T219

4			3				
SCOPOLETIN			LUTEOLIN				
PLIP (3D)	Protein Plus Zentrum (2D)		Chimera	PLIP (3D)	Protein Plus Zentrum (2D)		Chimera
N73, E70, V159	N73, E70, V159		K210	E70, N73, T77	E70, N73, T77		N211
F215$_{\Pi}$, S118, S217	F215$_{\Pi}$, S148, F215, V152		K210,T219,A226,G151,D147	N73, R155	N73, A115, E70, R80, T77		T77
E230, F215, A226	S118, F215$_{\Pi}$		N211,E70,N73	T77	N73, T77, D74, K210		E230
T113, N122, P121, N122				S217, F215, P216	S118, E230, S217, F215		
S114, A115, L116, Q233	Q233, L116			S118, T225, A226, V152	E230, T225, F215, D147, P216		R126
T113, M122			T219,N211	E70	Q218, N211, E70, D162		A226, T227
R106, S110			T65	N313, R76, P66, Y309	S310, L62, S314		G259
K283, W287	D267, W287, I271		S64	R76, N313, P 66	T65, L62, P66, P67, Y309		
T61	Q82		Q63	N313, R76, Q63	L62, P66, Y309, P67		D267
L166, K173	E197, L201, K204, L116		D74, K210	E70, N73, V159	N211, E70		D147

https://doi.org/10.25303/211rjbt2490261

	AFRORMOSIN					GINISTEIN							
6						5							
	Chimera	PLIP (3D)	Protein Plus Zentrum (2D)		Chimera	PLIP (3D)	Protein Plus Zentrum (2D)		Chimera				
	S118	S118, E230, F215, P216			A115	S217, E230, V152, F215, P216	W234, E230, F215, S148, S217						
	D147	S217, V152, F215, P216	A226, F215, P216, D147		A226,S217	V152, F215	E230, D147, P216, F215						
		Y309, N313	V157, T306, P67, Y309		P66,Q63	P66, S310, N313, Y309	N313, Y309, L62		S118, T227, S148, F117				
	Q218	S217	S217, P216, F215, T224		E154	S217, D147, R80, P216	S217, R80, T77		T113				
		Y309, T306, P66, N313	Y309, T306, L62			I145, T113, F117	T108, F109, I145						
	R106	P125, S110, R106	P125, S110, R106		A111,E103	E103, R106, P125, S110, M122	E103, R106, P125, S110						
	E197	A166, D169, L201			S310,L62	N313, S314, Y309, P66, R76	S310, S314, Y309, L62		R106, S110, A111				
	P112	T108, A111, I145, L319, T108, L315, S114	A111, T108, I145, L319, P112		N141	A111, S114, I145, L315	T108, A111, I145						
	Q63,S64	T306, R76, N313	T306, Y309, L62		Q294	E297, P260	N297, P260, E295		K54				
	S217	V152, D147	S148, F215		E230,S217, S148	S217, P216	S217, D147, S148, L116						

	BAPTIGENIN	Protein Plus Zentrum (2D)	D147, S214, S148, F215, E230,	L62, P67, P66	E103, P125, S110	S114, A111, F117	N297, G259, P260	L62, T65, Y309	S110, M122, P125	N313, S310, S314, Y309	Y309, L62	S120, M122, A111, N141
7		PLIP (3D)	F215, V152, S217, E230	P66, R76, N313, Y309	R106, S110, P112, A123	F117, A111, S114, I145, L315	P260, D257, N297	T306, N313, R76	S110, R106, P125	N313, S314, Y309	S310, R76, P66, Y309	N141, M122, T113
		Chimera	S148	Q63, S64	A123, Q124, E103	F109	N297	T306, S64, Y309, T65	T61		T306, T61, Q63	T113, F109

Blue: Hydrogen bonding; Orange: Hydrophobic bonding; Green Π-Π interactions

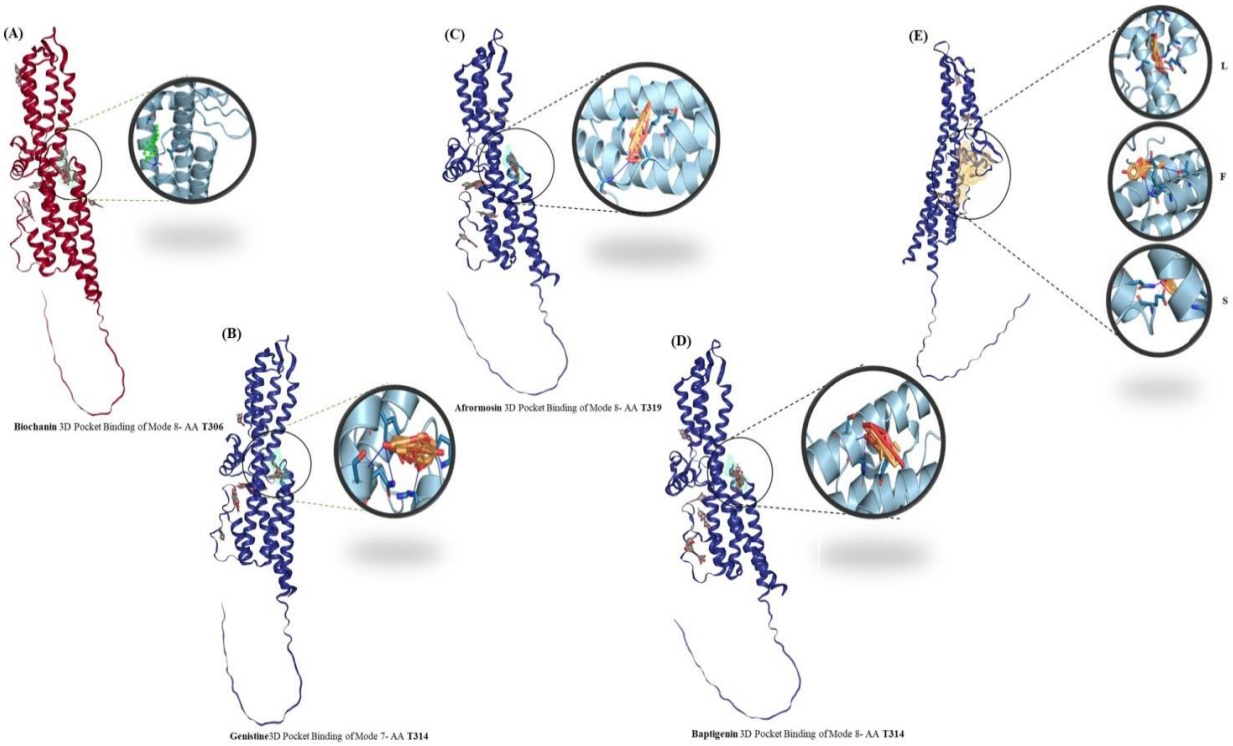

Figure 4: Depiction of 3D visualizations of the binding pocket for hydroxyisoflavones. In Cartoon structure of Sip protein showing binding with residue (A) Biochanin A binding in Mode 8 with amino acid residue T306 (B) Genistein binding in Mode 7 with amino residue S314, (C) Aforomosin in Mode 8 with amino acid residue L319, (D) Baptigenin in Mode 8 with amino residue S314, (E) Luteolin, Formononetin, Scopoletin in Mode 1 with amino acid residue E70, N73 interacting specifically with the amino acid residue, within the protein's active site. This representation highlights the ligand's orientation and key interactions within the binding pocket using visualization tool ProteinPlus (Zentrum) for protein Cartoon structure of Sip protein and 3D binding using PyMOL v3.1.3.

Table 3
Showcasing of Ligands binding with specific residues and their modes with compound structure and Lipinski parameters

S.N.	Compound	Structure	Lipinski's rule of five		Binding affinity residues (kcal/mol)	Active Amino acid Residue (distance in Å)
1	Biochanin A	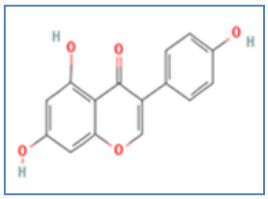	Molecular weight (<500DA)	268.26 g/mol	-7	
			XLogP(<5)	1.51		Amino Acid: **T306**
			H-Bond donor (5)	1		Distance : 3.72Å
			H-bond acceptor (<10)	4		
2	Genistein	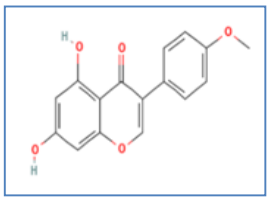	Molecular weight (<500DA)	270.24 g/mol	-6.7	
			XLogP(<5)	1.02		Amino Acid: **T306**
			H-Bond donor (5)	3		Distance: 3.34Å
			H-bond acceptor (<10)	5		
3	Baptigenin	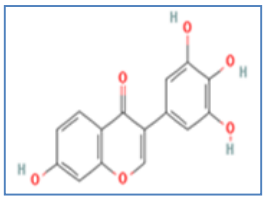	Molecular weight (<500DA)	286.24 g/mol	-6.6	
			XLogP(<5)	1.42		Amino Acid: **T306**
			H-Bond donor (5)	4		Distance: 3.01Å
			H-bond acceptor (<10)	6		
4	Afrormosin	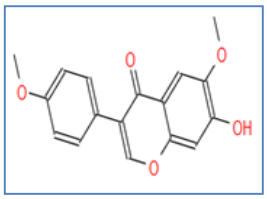	Molecular weight (<500DA)	298.29 g/mol	-6.5	
			XLogP(<5)	1.95		Amino Acid: **L319**
			H-Bond donor (5)	1		Distance: 3.53Å
			H-bond acceptor (<10)	5		

Discussion

Enteric fever, associated with *Salmonella Typhi* infection, is contributing significantly to foodborne illness in endemic regions[28]. Management of the disease is clinically done by use of antimicrobials[21]. However, empirical uses of antibiotics have exacerbated antimicrobial resistance (AMR), leading to challenges in effective disease management[3]. Recent reports suggest that *Salmonella* is acquiring resistance to conventional antibiotics, including fluoroquinolones, especially in developing nations of South-East Asia[14]. In a nutshell, novel antibiotics are the need of the hour for mitigation of the *Salmonella*-associated disease. Several attempts in the past have been made to discover newer antimicrobial drugs including naturally derived antimicrobials effective against the bug to address *Salmonella* linked AMR[6,15,24].

Additionally, these naturally derived compounds have an edge to the chemical or synthetic antimicrobials in terms of toxicity for their clinical applicability and offer an alternative avenue for drug discovery[28,38]. Thus, through the present study, attempts for novel antimicrobial discovery for potentially tagetting *Salmonella* sps were demonstrated through computational study. We have exploited the virulence factors associated with *Salmonella* type III secretion systems (T3SSs) which play an essential role in pathogenicity. We identified some of the target Sip proteins based on their degree of involvement for pathogenicity.

Therefore, we have targeted a receptor Sip protein (t2875) of *S. typhi* which is also present throughout the serovars and forms invasosomes.

Despite the availability of extensive protein structural data for *S. typhimurium* (a serovar associated with human infection, causing gastroenteritis), similar data for *S. typhi* remains limited. Additionally, crystal structure of the *Salmonella typhi*, t2875 protein was not yet available in the Protein Data Bank (PDB). However, research group from India, has recently attempted for crystallography of the SipD *S. typhi's* structure but there has been no formal PDB submission[13]. To overcome these limitations, sequence analysis of *S. typhi* and *S. typhimurium* (a closest serovar) and employing comparative homology modelling to study structural similarities and differences, we used Swiss-model to construct a predictive structural model of *S. typhi's* target Sip protein. The generated model allowed us to analyze homology, predict functional domains and identify potential drug target sites.

A virtual library of natural compounds was assembled based on their *in silico* pharmacokinetic properties including absorption, distribution, metabolism and excretion (ADME) through SwissADME and screened to identify seven potential candidates with promising pharmacokinetic profiles. Ligand docking studies on target Sip protein with defined grid aided in identifying key ligand-receptor interactions with the key compounds. Optimal binding conformations were selected based on docking scores and alignment. We utilised several web based tools viz. Protein-Ligand Interaction Profiler (PLIP), Protein Plus (zentrum), chimera for the commonality in key residue binding as well as specific binding pocket identification (Table 1 and 2, Figure 3 and 4).

The ligands' binding to these key residues of target Sip protein of *S. typhi* was hypothesized to disrupt the interaction of needle forming proteins in the invasosome assembly, one among the same being Prg1-SipD rearrangement, a critical structure required for host cell invasion. Molecular docking simulations revealed that four of the natural compounds from the current study, targeted critical residues within the Prg1-SipD coiled-coil interactions[25].

The binding of these ligands showed that these may potentially disrupt Prg1-SipD rearrangement necessary for the formation of the T3SS needle complex. Moreover, these findings were in concordance with earlier studies that highlighted the key residues' involvement as well as their importance in interactions for invasosome assembly and bacterial pathogenicity[25,31].

Thus, it underscores the value of leveraging natural products in combating antimicrobial resistance and developing effective, low-toxicity therapies for *Salmonella*-associated infections and their clinical management. However, the clinical translation of such agents requires rigorous *in vitro* and *in vivo* validation along with the optimization of their pharmacokinetic and pharmacodynamic properties.

Conclusion

Natural products are promising candidates for treating bacterial infections due to their low toxicity and potential to combat antimicrobial resistance. Hence, this study demonstrates a pipeline for the identification of potential natural compounds as alternate investigative drugs against *Salmonella* sps infections, by targeting the T3SS apparatus and Sip protein of *S. typhi*, for inhibiting formation of invasosomes, thereby impairing bacterial virulence.

Acknowledgement

CS received financial support as a research grants from Anusandhan National Research Foundation (ANRF) - Science and Engineering Research Board (SERB) under the State University Research Excellence (SURE) Scheme (SUR/2022/005545), Uttar Pradesh Higher Education Council (UPHEC - CoE and UPHEC R and D), India; and C.V. Raman grant from CSJM University. Authors are thankful to Chhatrapati Shahu Ji Maharaj University for providing research and development ecosystem.

References

1. Adasme M.F., Linnemann K.L., Bolz S.N., Kaiser F., Salentin S., Haupt V.J. and Schroeder M., PLIP 2021: expanding the scope of the protein-ligand interaction profiler to DNA and RNA, *Nucleic Acids Research*, **49**, W530-W534 **(2021)**

2. Anonymous UniProt: The Universal Protein Knowledgebase in 2025, *Nucleic Acids Research*, **53**, D609–D617 **(2024)**

3. Baker S., Thomson N., Weill F.X. and Holt K.E., Genomic insights into the emergence and spread of antimicrobial-resistant bacterial pathogens, *Science*, **360**, 733-738 **(2018)**

4. Browne A.J., Kashef Hamadani B.H., Kumaran E.A.P., Rao P., Longbottom J., Harriss E., Moore C.E., Dunachie S., Basnyat B., Baker S., Lopez A.D., Day N.P.J., Hay S.I. and Dolecek C., Drug-resistant enteric fever worldwide, 1990 to 2018: a systematic review and meta-analysis, *BMC Medicine*, **18**, 1 **(2020)**

5. Britto C.D., John J., Verghese V.P. and Pollard A.J., A systematic review of antimicrobial resistance of typhoidal Salmonella in India, *The Indian Journal of Medical Research*, **149**, 151-163 **(2019)**

6. Crump J.A., Sjolund-Karlsson M., Gordon M.A. and Parry C.M., Epidemiology, Clinical Presentation, Laboratory Diagnosis, Antimicrobial Resistance and Antimicrobial Management of Invasive Salmonella Infections, *Clinical Microbiology Reviews*, **28**, 901-937 **(2015)**

7. Daina A., Michielin O. and Zoete V., SwissADME: a free web tool to evaluate pharmacokinetics, drug-likeness and medicinal chemistry friendliness of small molecules, *Scientific Reports*, **7**, 42717 **(2017)**

8. Dahiya S., Sharma P., Kumari B., Pandey S., Malik R., Manral N., Veeraraghavan B., Pragasam A.K., Ray P., Gautam V., Sistla S.,

Parija S.C., Walia K., Ohri V., Das B.K., Sood S. and Kapil A., Characterisation of antimicrobial resistance in Salmonellae during 2014-2015 from four centres across India: An ICMR antimicrobial resistance surveillance network report, *Indian Journal of Medical Microbiology*, **35**, 61-68 **(2017)**

9. Derewenda U., Mateja A., Devedjiev Y., Routzahn K.M., Evdokimov A.G., Derewenda Z.S. and Waugh D.S., The structure of Yersinia pestis V-antigen, an essential virulence factor and mediator of immunity against plague, *Structure*, **12**, 301-306 **(2004)**

10. Erskine P.T., Knight M.J., Ruaux A., Mikolajek H., Wong Fat Sang N., Withers J., Gill R., Wood S.P., Wood M., Fox G.C. and Cooper J.B., High resolution structure of BipD: an invasion protein associated with the type III secretion system of Burkholderia pseudomallei, *Journal of Molecular Biology*, **363**, 125-136 **(2006)**

11. Fahrrolfes R., Bietz S., Flachsenberg F., Meyder A., Nittinger E., Otto T., Volkamer A. and Rarey M., ProteinsPlus: a web portal for structure analysis of macromolecules, *Nucleic Acids Research*, **45**, W337-W343 **(2017)**

12. Galan J.E., Salmonella interactions with host cells: type III secretion at work, *Annual Review of Cell and Developmental Biology*, **17**, 53-86 **(2001)**

13. Gopinath S.P.P., Raina R., Arockiasamy A. and Sundarabaalaji N., Crystallization and X-Ray Diffraction Studies of Salmonella Invasion Protein D (SipD), Insight Tip Component of Salmonella typhi Type III Secretion System, *Crystallography Reports*, **64**, 1108-1111 **(2019)**

14. Hakanen A., Kotilainen P., Huovinen P., Helenius H. and Siitonen A., Reduced fluoroquinolone susceptibility in Salmonella enterica serotypes in travelers returning from Southeast Asia, *Emerging Infectious Diseases*, **7**, 996-1003 **(2001)**

15. Threlfall E.J., Antimicrobial drug resistance in Salmonella: problems and perspectives in food- and water-borne infections, *FEMS Microbiology Reviews*, **26**, 141-148 **(2002)**

16. Irwin J.J., Tang K.G., Young J., Dandarchuluun C., Wong B.R., Khurelbaatar M., Moroz Y.S., Mayfield J. and Sayle R.A., ZINC20-A Free Ultralarge-Scale Chemical Database for Ligand Discovery, *Journal of Chemical Information and Modeling*, **60**, 6065-6073 **(2020)**

17. Johnson S., Roversi P., Espina M., Olive A., Deane J.E., Birket S., Field T., Picking W.D., Blocker A.J., Galyov E.E., Picking W.L. and Lea S.M., Self-chaperoning of the type III secretion system needle tip proteins IpaD and BipD, *The Journal of Biological Chemistry*, **282**, 4035-4044 **(2007)**

18. Kim S., Chen J., Cheng T., Gindulyte A., He J., He S., Li Q., Shoemaker B.A., Thiessen P.A., Yu B., Zaslavsky L., Zhang J. and Bolton E.E., PubChem 2023 update, *Nucleic Acids Research*, **51**, D1373-D1380 **(2023)**

19. Kubori T. et al, Supramolecular structure of the Salmonella typhimurium type III protein secretion system, *Science*, **280**, 602-605 **(1998)**

20. Klemm E.J., Shakoor S., Page A.J., Qamar F.N., Judge K., Saeed D.K., Wong V.K., Dallman T.J., Nair S., Baker S., Shaheen G., Qureshi S., Yousafzai M.T., Saleem M.K., Hasan Z., Dougan G. and Hasan R., Emergence of an Extensively Drug-Resistant Salmonella enterica Serovar Typhi Clone Harboring a Promiscuous Plasmid Encoding Resistance to Fluoroquinolones and Third-Generation Cephalosporins, *mBio*, **9**, e00105-18 **(2018)**

21. Kuehn R., Stoesser N., Eyre D., Darton T.C., Basnyat B. and Parry C.M., Treatment of enteric fever (typhoid and paratyphoid fever) with cephalosporins, *The Cochrane Database of Systematic Reviews*, **11**, CD010452 **(2022)**

22. Lara-Tejero M. and Galan J.E., Salmonella enterica serovar typhimurium pathogenicity island 1-encoded type III secretion system translocases mediate intimate attachment to nonphagocytic cells, *Infection and Immunity*, **77**, 2635-2642 **(2009)**

23. Lou L., Zhang P., Piao R. and Wang Y., Salmonella Pathogenicity Island 1 (SPI-1) and Its Complex Regulatory Network, *Frontiers in Cellular and Infection Microbiology*, **9**, 270 **(2019)**

24. Liljebjelke K.A., Hofacre C.L., White D.G., Ayers S., Lee M.D. and Maurer J.J., Diversity of Antimicrobial Resistance Phenotypes in Salmonella Isolated from Commercial Poultry Farms, *Frontiers in Veterinary Science*, **4**, 96 **(2017)**

25. Lunelli M., Hurwitz R., Lambers J. and Kolbe M., Crystal structure of PrgI-SipD: insight into a secretion competent state of the type three secretion system needle tip and its interaction with host ligands, *PLoS Pathogens*, **7**, e1002163 **(2011)**

26. Marlovits T.C., Kubori T., Sukhan A., Thomas D.R., Galan J.E. and Unger V.M., Structural insights into the assembly of the type III secretion needle complex, *Science*, **306**, 1040-1042 **(2004)**

27. Neupane D.P., Dulal H.P. and Song J., Enteric Fever Diagnosis: Current Challenges and Future Directions, *Pathogen*, **10**, 410-426 **(2021)**

28. Newman D.J. and Cragg G.M., Natural Products as Sources of New Drugs from 1981 to 2014, *Journal of Natural Products*, **79**, 629-661 **(2016)**

29. Parry C.M., Hien T.T., Dougan G., White N.J. and Farrar J.J., Typhoid fever, *The New England Journal of Medicine*, **347**, 1770-1782 **(2002)**

30. Pettersen E.F., Goddard T.D., Huang C.C., Couch G.S., Greenblatt D.M., Meng E.C. and Ferrin T.E., UCSF Chimera--a visualization system for exploratory research and analysis, *Journal of Computational Chemistry*, **25**, 1605-1612 **(2004)**

31. Rathinavelan T., Tang C. and De Guzman R.N., Characterization of the interaction between the Salmonella type III secretion system tip protein SipD and the needle protein PrgI by paramagnetic relaxation enhancement, *The Journal of Biological Chemistry*, **286**, 4922-4930 **(2011)**

32. Sharma C. et al, A repertoire of high-affinity monoclonal antibodies specific to S. typhi: as potential candidate for improved typhoid diagnostic, *Immunologic Research*, **62**, 325-340 **(2015)**

33. Sharma T., Sharma C., Sankhyan A., Bedi S.P., Bhatnagar S., Khanna N., Gautam V., Sethi S., Vrati S. and Tiwari A., Serodiagnostic evaluation of recombinant CdtB of S. Typhi as a

potential candidate for acute typhoid, *Immunologic Research*, **66**, 503-512 **(2018)**

34. Schoning-Stierand K., Diedrich K., Ehrt C., Flachsenberg F., Graef J., Sieg J., Penner P., Poppinga M., Ungethum A. and Rarey M., ProteinsPlus: a comprehensive collection of web-based molecular modeling tools, *Nucleic Acids Research*, **50**, W611-W615 **(2022)**

35. Schoning-Stierand K., Diedrich K., Fahrrolfes R., Flachsenberg F., Meyder A., Nittinger E., Steinegger R. and Rarey M., ProteinsPlus: interactive analysis of protein-ligand binding interfaces, *Nucleic Acids Research*, **48**, W48-W53 **(2020)**

36. Tailor Hetal, Limbachiya Pruthviraj and Mahajan Dharmesh H., Three components: one-pot synthesis of tetrazoles using silica-supported melamine tri-sulfonic acid, an efficient and reusable heterogeneous catalyst, *Res. J. Chem. Environ.*, **28(4)**, 88-96 **(2024)**

37. Waterhouse A., Bertoni M., Bienert S., Studer G., Tauriello G., Gumienny R., Heer F.T., De Beer T.A.P., Rempfer C., Bordoli L., Lepore R. and Schwede T., SWISS-MODEL: homology modelling of protein structures and complexes, *Nucleic Acids Research*, **46**, W296-W303 **(2018)**

38. Xavier J.B., Sociomicrobiology and Pathogenic Bacteria, *Microbiology Spectrum*, **4(3)**, VMBF-0019-2015 **(2016)**.

(Received 10th Febraury 2025, accepted 15th April 2025)